Bulletin of Faculty of Science, Zagazig University (BFSZU)
e-ISSN: 1110-1555
Volume-2023, Issue-2, pp-33-41
https://bfszu.journals.ekb.eg/journal
Research Paper DOI: 10.21608/bfszu.2023.172352.1198

==========

Optical analysis of Hybrid quantum dots deposited by SILAR method

Asmaa F. Mansour[1], Sawsan A. Mahmoud[2], and Moustafa E.Elsisi[1]

[1]Zagazig University, Physics department, Faculty of science, Zagazig, Egypt.
[2]Egyptian Petroleum Research Institute, postal code 11727, Nasr City, Cairo, Egypt.
Corresponding Author: Moustafa E.Elsisi; mostafaels999@gmail.com

ABSTRACT: **In the present study, ZnS and CdS quantum dots (QDs) are attached to mesoporous titanium film by successive ionic layer adsorption and reaction to the synthesized three layers of ZnS and CdS quantum dots (QDs) to form ZnS/TiO_2 nanocomposites (NCs), CdS/TiO_2, and CdS/ZnS/TiO_2 (NCs) as hybrid structures. TiO_2 nanoparticles (NPs) are fabricated by the sol-gel method. The synthesized nanomaterials were investigated by XRD, HR-TEM, FTIR, and UVVisible spectrophotometer. The size of TiO_2 NPs was investigated from XRD analysis to be 34.33 nm and was confirmed with HR-TEM. The UV–Vis absorption spectra for samples were recorded. The optical band gap energies (Eg) have been calculated for the deposited films and were found to be 2.39 eV, 2.30 eV, 1.98 eV, and 1.68 eV for TiO_2 NPs, ZnS/TiO_2, CdS/ TiO_2, and/CdS/ZnS/ TiO2 NCs, respectively.**

KEYWORDS: Sol-gel method; SILAR method; CdS QDs; TiO_2 NPs; **Hybrid structures.**

Date of Submission: 08-11-2022 Date of acceptance: 08-03-2023

I. INTRODUCTION

One-dimensional nanostructures, such as nanorods, nanowires, and nanotubes, exhibit interesting electrical and optical properties due to the quantum confinement effect and low dimensionality. Realizing the field of radiation with nano-science promotes wide opportunities in the field of photonics, radiation detectors, photo detectors, and in sensing applications [6-8]. Cadmium sulphide is the most essential II-VI n-type compound semiconductor because of its eminent properties such as nonlinear piezoelectricity, good thermal and chemical stability, optical behavior, direct band gap, and optical coefficient. Onedimensional CdS quantum dots contain several properties, such as a high aspect ratio, efficient transport properties, and so on, resulting in next-generation nanoscale electronic and photonic devices. One dimensional CdS quantum dots are distinguished materials for photovoltaic cells, nonlinear optics, optoelectronic devices, sensors, and photocatalytic applications [9-10]. Different methods, such as chemical bath deposition [15], spin coating [11], chemical vapor deposition (CVD) [12], and chemical dip coating [4] have been used to form semiconducting thin films. In the current work, CdS and ZnS thin films are deposited on the glass substrate using the SILAR method because it is a simple, efficient, and cost effective technique. The optical properties of semiconducting nanostructures can be modified by using a number of methods such as ion doping, irradiation, and ion implantation. The refinement in the optical properties such as the band gap is pretended due to the generation of impurity levels in the forbidden energy gap [3].

QDs are nanocrystalline materials that have a size in the range of 2 to 10 nm and have perfect photostability as well as large extinction coefficients [20]. Interestingly, QDs have received much awareness in the growth of solar cell technologies because of the quantum confinement effect that they display as their exciton Bohr radius decreases. A QD with a smaller size than its exciton Bohr radius is said to have strong custody, whereas a QD with a larger size than its exciton Bohr radius is said to have a weak quantum custody effect. QDs absorb and emit precise color at a specific spectral wavelength corresponding to their particle sizes. Generally, the smaller QDs emit blue light, while the largest nanosized QDs emit red light, with all the other colors appearing in between. This color-changing phenomenon indicates that QDs of a certain particle size take possession of specific optoelectronic properties and differ in terms of their bandgap energies. The bandgap is the required energy to raise the electrons from the (V.B) to (C.B). Theoretically, small-sized dots have a higher energy gap

than their bulk counterparts and require energy equal to or higher than their bandgap energy to enter an excited state. The discipline of QD particle size, energy level, and emission wavelength makes them extremely useful for optoelectronic applications such as photovoltaic cells [16-18] and sensors [21-30]. The successive ionic layer adsorption and reaction (SILAR) is the preferred technique for the adsorption of CdS and ZnS QDs on TiO2 NPs. This work focuses on the processing of QDs based on the SILAR method, and optical properties of hybrid structures are discussed corresponding to their bandgap energy and spectral absorption [2]. Most research has focused on engineering the device structure [39, 40] and functionalizing QD surfaces to improve the performance of QD-based LEDs [41, 42, 43].

In our work, the effect of different quantum dots on the optical behavior of TiO2 NPs is further investigated, which is more importantly associated with ZnS over TiO2 QDs, CdS over TiO2 and hybrid structures of CdS and ZnS over TiO2. The optical energy gap of TiO2 was studied after the deposition of ZnS, CdS, and CdS/ZnS at 50 °C. 3- Environmental factors

II. MATERIALS AND METHODS

Apparatus

(Titanium (IV) isopropoxide (97%, Aldrich), Zinc Acetate Zn (CH3COO) 2 (97%, Bio Chem), Sodium Sulfide Na2S (98%, Alpha chemical), Cadmium Nitrate Cd (NO3)2 (97%, Bio Chem), Ethanol absolute (99%, Bio Chem), Triton -X100 (97%, Aldrich), (FTO conducting glass).

2.1. Synthesis of TiO2 nanoparticle by Sol-gel method:

TiO2 NPs were prepared by a sol-gel approach using Titanium (IV) isopropoxide (TIP) [Ti [OCH (CH3)2]4 as a precursor according to [8]. The sol-gel method includes the condensation and hydrolysis processes of titanium (IV) isopropoxide in aqueous media under acidic conditions. The procedure used is followed by preparing two solutions: In solution (1), TIP was added to absolute ethanol at a ratio of one to three by volume under continuous stirring for 30 minutes until a homogenous clear yellow solution formed. Solution (2) contains DI water and absolute ethanol at a volume ratio of one to four. Then, HNO3 as N2 atmosphere is mixed well into the solution by dropwise addition until the pH value approaches about 2 under continuous stirring for 1 h at room temperature to restrain the hydrolysis process of the solution. Finally, solution 2 was added slowly to solution 1 and aged under robust stirring for 2 h. The gel was digested at 80 ºC in water path for 1 h until most of the ethanol evaporated, then dried for 24 h in a regular laboratory oven at 80ºC and then calcined at 400 ºC for 2 h [33].

2.2. Thin films preparation

A TiO2 NPs film with the same thickness of 0.0051g/cm2 was prepared. The samples of TiO2 NPs film were directly deposited onto glass substrates by the doctor-blading method. Before spreading the film, the glass sheet surfaces were cleaned for 30-60 min using an ultrasonicator, then dried in air. To produce the film of TiO2 NPs, the powder was first dispersed in TritonX100, acetic acid, and ethanol until it became a homogeneous paste nanomaterial. The paste was spread on the glass surface using a glass slide, and then the suspended powder was added as drops in the middle of the substrate and spread to form a thick film. The layer was then kept at room temperature for 30 minutes before being dried on a hot plate at 300 oC for 5 min [33].

2.3. Synthesis of ZnS/TiO2, CdS/TiO2, and CdS/ZnS/TiO2 nanocomposites as a hybrid structure:

The ZnS and CdS QDs act as light absorbers by the Successive Ionic Layer Adsorption and Reaction (SILAR) method. For the growth of ZnS QDs, the TiO2 semiconductor film was initially immersed in a 0.2 M Zn (CH3COO)2 aqueous solution for 2 min and then rinsed off with ethanol to remove excess ions and dried on a hot plate at 60 ºC for 1 min. Then, the film was dipped into a 0.2 M Na2S aqueous solution for another 2 min to allow S2- to react with the preadsorbed Zn2+, leading to the formation of ZnS QDs. The loosely bound S2- ions were removed by rinsing the film in methanol, and then the film was dried at 60 ºC for 1 min. The entire procedure is termed as one cycle, and the incorporated amount of ZnS can be increased by increasing the number of cycles to 3 cycles The films with different cycles were calcined at 300 ºC for 5 min at a high temperature to increase the crystallinity of ZnS QDs [2]. The TiO2 semiconductor film was immersed in a 0.2 M Cd (NO3)2 aqueous solution for 2 min before being rinsed with ethanol and dried for 1 min on a hot plate at 60 oC. Then, the film was dipped into a 0.2 M Na2S aqueous solution for another 2 min to allow S2- to react with the pre-adsorbed Zn2+, leading to the formation of CdS QDs. The loosely bound S2-ions were removed by rinsing the film in methanol, and then the film was dried at 60 ºC for 1 min. The entire procedure is termed as one cycle, and the incorporated amount of CdS can be increased by increasing the number of cycles to 3 cycles.

To increase the crystallinity of CdS QDs, the films with different cycles were calcined at 300 oC for 5 min [7]. To grow a ZnS/CdS hybrid structure on TiO2, immerse the TiO2 film in a 0.2 M Zn(CH3CO)2 aqueous solution for 2 min, then rinse with ethanol to remove excess ions before drying for 1 min on a hot plate at 60 oC. Then, the film was dipped into a 0.2 M Na2S aqueous solution for another 2 min to allow S2- to react with the pre-adsorbed Zn2+, leading to the formation of ZnS QDs. This was followed by immersing the film of TiO2/ZnS into a 0.2 M Cd (NO3)2 aqueous solution for 2 min, rinsed off with ethanol to remove excess ions, and dried on a hot plate at 60 ºC for 1 min. Then, the film was dipped into a 0.2 M Na2S aqueous solution for another 2 min to allow S2- to react with the pre-adsorbed Zn2+, leading to the formation of CdS/ZnS hybrid QDs [7].

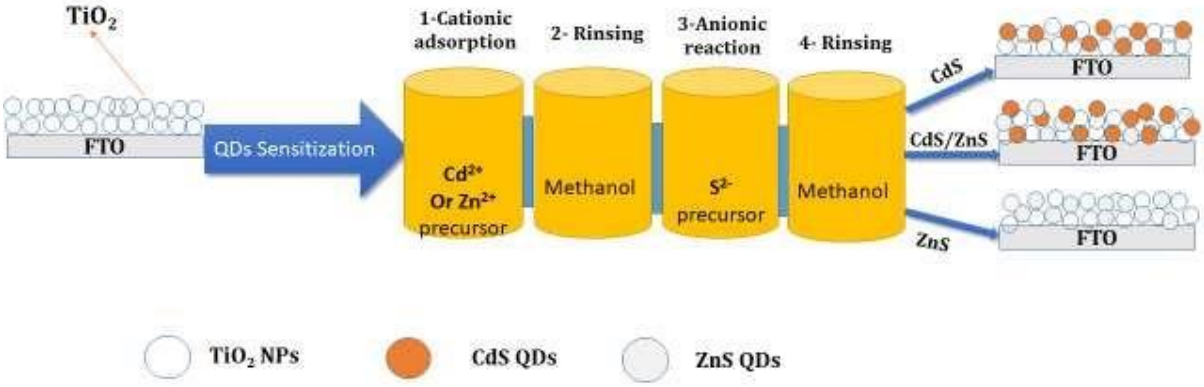

Schematic diagram of quantum dot deposition by SILAR Method

2.4. Methods of Analysis:

Several techniques were used to characterize the surface of prepared materials. X-ray diffraction patterns were reported using a Pan Analytical Model X 'Pert Pro, which was fitted with CuKα radiation (α = 0.1542 nm), Ni-filter, and general area detector. A 40 kV accelerating voltage and a 40 mA emission current were utilized. In the 2θ from 0.5–70o range, the diffract grams were registered. The Fourier transform infrared spectroscopy (FT-IR) of the prepared samples was measured using the KBr technique adopted by the Nicolet Is-10 FT-IR spectrophotometer (Thermo Fisher Scientific). The KBr technique was conducted roughly in a quantitative manner for all samples, since the sample weight and that of KBr were both held constant. A Field Emission Scanning Electron Microscope (FE-SEM) is used to examine the material's composition, particle size, and shape. For the samples prepared, a 30 kV acceleration voltage operating on a JSM-7500F electron microscope was reported. The optical absorption spectra of the samples were analyzed using Ultraviolet-Visible absorption spectroscopy (Spectro UV-Vis 2800, United States).

III. RESULTS

XRD analysis was applied for the determination of purity, crystallinity, and crystalline size. The XRD pattern spectra of the TiO2 NPs calcined at 400oC is depicted in Figure 1 (a). The XRD spectra of three samples show that the anatase phases are formed with the sharp peaks for TiO2 NPs. All diffraction peaks for the sample were congruent with the tetragonal structure of TiO2 NPs anatase phase and all diffraction peaks were in good agreement with JCPDS No. 21-1272. The diffraction angle peaks existing at 2θ = 25.210, 37.600, 47.940, 51.450, 53.920, 55.010, 62.590 and 65.420 correspond to the (101), (004), (200), (105), (211), (204), (116), and (215) lattice planes respectively. As shown in Fig. 1 (b), the pattern of the cubic phase of CdS, with preferred

orientation along the (111) direction at 2θ = 26.66◦ [32]. This preferred orientation is frequently reported in SILAR-prepared CdS thin films [1, 6].A small contribution of the planes of cubic CdS at 2θ = 44.03◦ is also observed [7]. Both XRD-peaks were indexed in the crystallography open database entry COD-1011251. The CdS sample exhibits with minor intensity the (100) at 2θ = 24.83◦ and (1 1 1) at 28.22◦ reflections of the hexagonal CdS phase (COD-1011054). A cubic structure of zinc sulphide QDs was identified from the XRD patterns in Fig. 1 (c) in which the peak positions of ZnS (JCPDS 65-9585) are shifted slightly too large as compared with the TiO2 NPs and CdS QDs [18]. The Sherrer equation was used to calculate the average crystallite size, which is as follows:

$$D = K\lambda/\beta\cos\theta \qquad (1)$$

Where: D is the crystallite size; K is a dimensionless shape factor, has a typical value of about 0.9 nm, λ=1.54A° is the X-ray wavelength; β is the broadening full width at half the maximum intensity (FWHM); and θ is the Bragg's diffraction angle [36].

The crystallite size of the pure TiO2 NPs, CdS QDs, and ZnS QDs nanostructures is shown in the below Table1.

Table 1: Crystallite Size, Thickness and Eg of pure nanostructures.

Nanostructures	Crystallite size (nm)	Eg (eV)	Thickness (cm)
TiO_2	11.80	2.39	0.0051
ZnS	25.91	2.25	0.01
CdS	10.3	2.2	0.013

Figure 2 shows the FTIR spectra curves of (a)-TiO2 NPs, (b)-CdS QDs, and (c)-ZnS QDs.

Figure 2(a) shows the FTIR spectra for sample TiO2 NPs calcined at 400oC and shows that the absorption band observed in the ranges of 400 confirms to 800 cm−1 is associated to the bending vibration (O-Ti-O) bonds in the TiO2 lattice [36-37], which indicates the presence of TiO2 as a crystalline phase. The sharp peak at 1620 cm−1 refers to the characteristic bending vibration of the OH group [38-39]. A broad absorption peak observed in the range of 3200 to 3800 cm−1 is due to the interaction of the hydroxyl group of water molecules with the TiO2 surface [36-37]. Fig. 2 (b) shows a very small related peak because CdS possesses a broad absorption band in the far infrared region. Also, Fig. 2(c) shows the sharp peaks, functional groups, and absorption peaks of ZnS QDs. The formation of ZnS QDs is confirmed by it. Figure 3 shows the FE-SEM images for the TiO2 QDs, CdS QDs, and ZnS QDs. From FE-SEM images of samples, Fig.3 (a), it is found the particles for TiO2 QDs are homogeneous and almost irregular in shape. It is found that particle size is increased and is highly agglomerated at 11.8 nm. Fig.3 (b) shows the micrographs of ZnS QDs, ZnS QDs are spherical shapes with a uniform of about 93.80 nm, and Fig.3 (c) shows that CdS QDs morphology and indicates an average size of about 14.21 nm.

Figure 4 shows the optical absorption spectra of UV–vis for TiO2 NPs, TiO2/ZnS NCs, TiO2/CdS NCs and TiO2/CdS/ZnS NCs respectively. The spectrum of the quantum dots deposition is different than the spectrum of TiO2 NPs, where the optical absorbance of TiO2/CdS/ZnS NCs is higher than TiO2 NPs, TiO2/ZnS NCs and TiO2/CdS NCs. which confirmed that the TiO2/CdS/ZnS NCs have a maximum absorbance.

To know the optical band gap, we have made a detailed calculation of the band gap using the Tauc formula; (αhν) =A (hυ - Eg)n, here, α is the absorption coefficient, hυ is the photon energy, and Eg is the energy gap, and n indicates the quality of the transitions. The term n is taken to be 2 for a direct transition and ½ for an indirect transition. The optical bandgap energy is investigated by plotting (αhυ) 1/n versus photon energy and drawing the tangent to the curve that intersects with the energy axis at α = 0. Fig.5 shows the Tauc plot of TiO2 NPs, TiO2/ZnS NCs, TiO2/CdS NCs and TiO2/CdS/ZnS NCs for direct transition and the estimated energy gaps of TiO2 NPs, TiO2/ZnS NCs, TiO2/CdS NCs and TiO2/CdS/ZnS NCs are 2.39 eV, 2.30 eV, 1.98 eV and 1.68 eV,

III. RESULTS

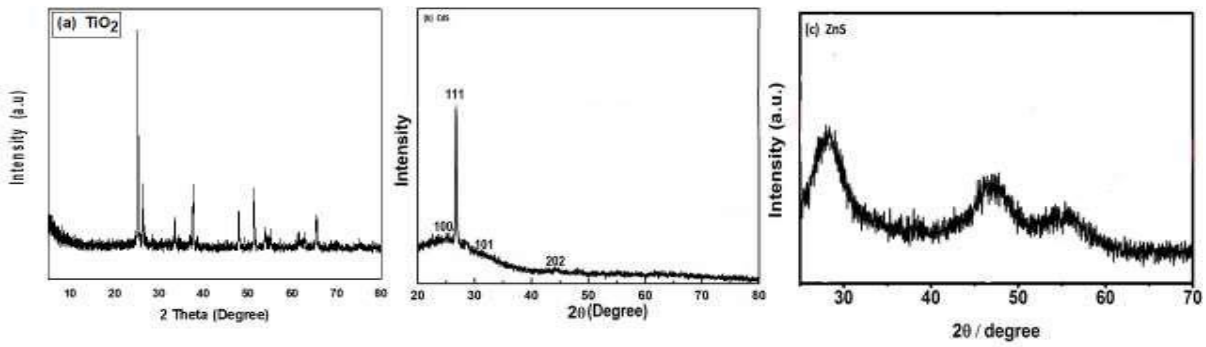

Figure1: XRD spectra of (a)-TiO_2 NP_s, (b)-CdS QD_s and (c)-ZnS QD_s.

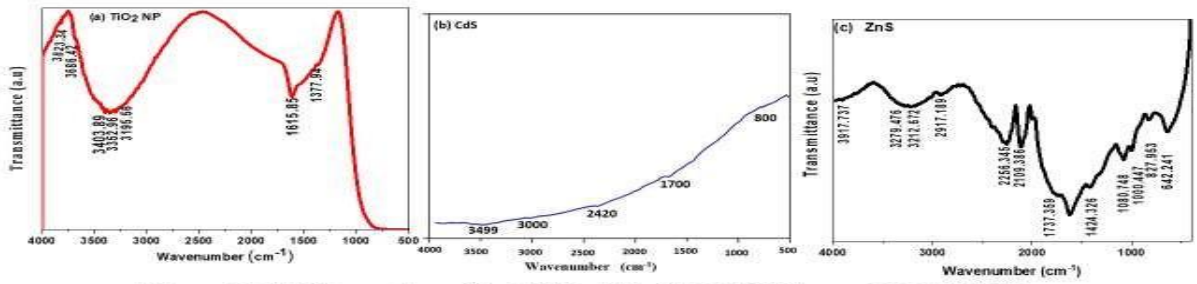

Figure2: FTIR spectra of (a)-TiO_2 NP_s, (b)-CdS QD_s and (c)-ZnS QD_s.

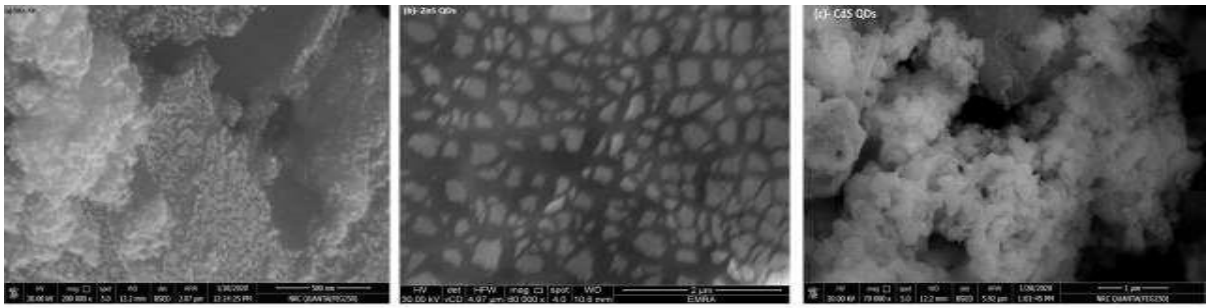

Figure 3: FE-SEM of nanostructures (a)-TiO2 NP_s, (b)-ZnS QD_s and (C)-CdS QD_s.

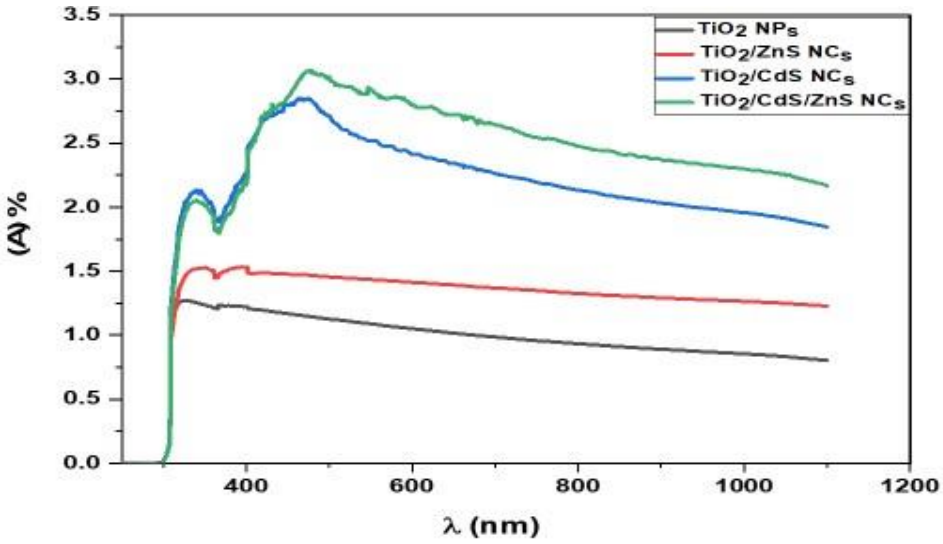

Figure 4: Absorbance spectra of the TiO_2 NP_s, TiO_2/ZnS NC_s, TiO_2/CdS NC_s and TiO_2/CdS/ZnS NC_s.

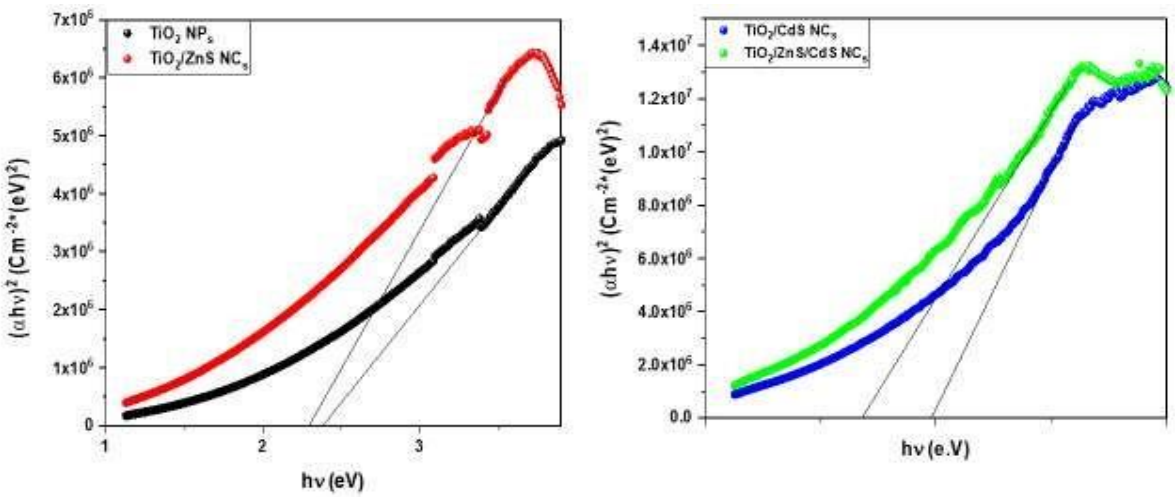

Figure 5: Optical band gap of the TiO2 NP_s, TiO2/ZnS NC_s, TiO_2/CdS NC_s and TiO_2/CdS/ZnS NC_s.

IV. CONCLUSION

A TiO_2 nanoparticle was successfully synthesized by a sol-gel method. The TiO_2/ZnS, TiO_2/CdS, and TiO_2/CdS/ZnS nanocomposites were successfully synthesized by the SILAR method. We found that the particle size of CdS QDs is smaller than TiO_2 NPs and ZnS QDs and the absorbance of TiO2 NPs was increasing by quantum dot deposition under UV-irradiation (TiO_2/CdS/ZnS< TiO_2/CdS <TiO_2/ZnS <TiO_2 NPs(. Optical band gap energy in direct allowed transition for TiO2 NPs was decreased by adsorption of different quantum dots on the surface of TiO_2 to form hybrid structures where (Eg) for TiO_2/CdS/ZnS is lower than Eg of TiO_2/CdS NCs, TiO_2/ZnS, and TiO_2NPs. This means that deposition of hybrid quantum dots is the

most efficient nanocomposites as a semiconducting nanomaterial and can be used as a photoanode in quantum dot sensitized solar cells (QDSSCs).

REFERENCES

Jaya Khatter, R.P. Chauhan: Gamma-ray induced modifications on CdS nanorod mesh:Structural, optical, and electrical properties, Radiation Physics and Chemistry **182** (2021) 109353.

Nurul Syafiqah Mohamed Mustakim, Charles Ahamefula Ubani, Suhaila Sepeai, Norasikin Ahmad Ludin, Mohd Asri Mat Teridi, Mohd Adib Ibrahim: Quantum dots processed by SILAR for solar cell applications, Solar Energy **163** (2018) 256–270.

Ali, S.M., Ramay, S.M., Rehman, N.U., Al Khuraiji, T.S., Shar, M.A., Mahmood, A., Riaz, M., 2019: Investigation of gamma irradiation effects on the properties of CdS/ p-Si heterostructure. Mater. Sci. Semicond. Process. 93, 44–49.

Dhatchinamurthy, L., Thirumoorthy, P., Arunraja, L., Subramanian, R., 2019.: Effect of annealing temperature on the structural and optical properties of CdS/PVA nanostructure thin films using dip coating method. J. Cluster Sci. **30** (3), 827–835.

Cheng, L., Xiang, Q., Liao, Y., Zhang, H., 2018: CdS-based photocatalysts. Energy Environ. Sci. **11** (6), 1362–1391.

Kumar, P., Saxena, N., Dewan, S., Singh, F., Gupta, V., 2016: Giant UV-sensitivity of ion beam irradiated nanocrystalline CdS thin films. RSC Adv. **6** (5), 3642–3649.

Kumar, S., Kumar, M.V., Pattabi, M., Asokan, K., Chandrashekar, B.N., Chun, C., Krishnaveni, S., 2018: Effect of gamma irradiation on electrical properties of CdTe/ CdS solar cells. Mater Today-Proc **5** (10), 22570–22575.

Nikfarjam, A., Salehifar, N., 2015: Improvement in gas-sensing properties of TiO2 nanofiber sensor by UV irradiation. Sensor. Actuator. B Chem. 211, 146–156.

Deng, K., Li, L., 2014: CdS nanoscale photo-detectors. Adv. Mater. **26** (17), 2619–2635.

Kang, Y., Kim, D., 2006: Well-aligned CdS nanorod/conjugated polymer solar cells. Sol. Energy Mater. Sol. Cells **90** (2), 166–174.

Wu, K.J., Chu, K.C., Chao, C.Y., Chen, Y.F., Lai, C.W., Kang, C.C., Chou, P.T., 2007: CdS nanorods imbedded in liquid crystal cells for smart optoelectronic devices. Nano Lett. **7** (7), 1908–1913.

Buckingham, M.A., Catherall, A.L., Hill, M.S., Johnson, A.L., Parish, J.D., 2017: Aerosol-assisted chemical vapor deposition of CdS from xanthate single source precursors. Cryst. Growth Des. **17** (2), 907–912.

Ahn, S., Lin, Y.H., Ren, F., Oh, S., Jung, Y., Yang, G., Pearton, S.J., 2016: Effect of 5 MeV proton irradiation damage on performance of β-Ga2O3 photo detectors. J. Vac. Sci. Technol., B **34** (4), 041213.

Slonopas, A., Ryan, H., Foley, B., Sun, Z., Sun, K., Globus, T., Norris, P., 2016: Growth mechanisms and their effects on the opto-electrical properties of CdS thin films prepared by chemical bath deposition. Mater. Sci. Semicond. Process. 52, 24–31.

Lee, J.C., Kim, T.G., Lee, W., Han, S.H., Sung, Y.M., 2009: Growth of CdS nanorod coated TiO2 nanowires on conductive glass for photovoltaic applications. Cryst. Growth Des. **9** (10), 4519–4523.

Hod, I., Zaban, A., 2014: Materials and interfaces in quantum dot sensitized solar cells: challenges, advances and prospects. Langmuir 30, 7264–7273.

Chang, J., Oshima, T., Hachiya, S., Sato, K., Toyoda, T., Katayama, K., Hayase, S., Shen, Q., 2015: Uncovering the charge transfer and recombination mechanism in ZnS coated PbS quantum dot sensitized solar cells. Sol. Energy 122, 307–313.

Kamat, P.V., 2013: Quantum dot solar cells. The next big thing in photovoltaics. J. Phys. Chem. Lett. 4, 908–918.

Kamat, P.V., Christians, J.A., Radich, J.G., 2014: Quantum dot solar cells: hole transfer as a limiting factor in boosting the photoconversion efficiency. Langmuir 30, 5716– 5725.

Kouhnavard, M., Ikeda, S., Ludin, N.A., Ahmad Khairudin, N.B., Ghaffari, B.V., Mat- Teridi, M.A., Ibrahim, M.A., Sepeai, S., Sopian, K., 2014: A review of semiconductor materials as sensitizers for quantum dot-sensitized solar cells. Renew. Sustain. Energy Rev. 37, 397–407.

Li, H., Jiao, S., Li, H., Li, L., Zhang, X., 2015: Tunable growth of PbS quantum dot– ZnO heterostructure and mechanism analysis. CrystEngComm 17, 4722–4728.

Li, H., Wang, C., Peng, Z., Fu, X., 2015b: A review on the synthesis methods of CdSe Sbased nanostructures. J. Nanomater. 1–16.

Li, L., Xiao, J., Yang, X., Zhang, W., Zhang, H., 2015c: High efficiency CdS quantum dot sensitized solar cells with boron and nitrogen co-doped TiO2 nano film as effective photoanode. Electrochim. Acta 169, 103–108.

Li, T.-L., Lee, Y.-L., Teng, H., 2012: High-performance quantum dot-sensitized solar cells based on sensitization with CuInS2 quantum dots/CdS heterostructure. Energy Environ. Sci. 5, 5315.

Li, W., Pan, Z., Zhong, X., 2015d: CuInSe2 and CuInSe2-ZnS based high efficiency "Green" quantum dot sensitized solar cells. Mater. Chem. A 3, 1649–1655.

Li, Y., Wei, L., Wu, C., Liu, C., Chen, Y., Liu, H., Jiao, J., Mei, L., 2014a: Flexible quantum dot-sensitized solar cells with improved efficiencies based on woven titanium. J. Mater. Chem. A Mater. Energy Sustain. 2, 15546–15552.

Li, Z., Wang, Y., Ni, Y., Kokot, S., 2015e: A sensor based on blue luminescent graphene quantum dots for analysis of a common explosive substance and an industrial intermediate, 2,4,6-trinitrophenol. Spectrochim. Acta – Part A Mol. Biomol. Spectrosc. 137, 1213–1221**.**

Li, Z., Yu, L., Liu, Y., Sun, S., 2014b: Enhanced photovoltaic performance of solar cell based on front-side illuminated CdSe/CdS double-sensitized TiO_2 nanotube arrays electrode. J. Mater. Sci. 49, 6392–6403.

Wu, P., Ou, K., Chen, J., Fang, H., 2014: Methotrexate-conjugated AgInS2/ZnS quantum dots for optical imaging and drug delivery. Mater. Lett. 128, 412–416.

Mozafari, M., Moztarzadeh, F., 2011: Microstructural and optical properties of spherical lead sulphide quantum dots-based optical sensors. Micro Nano Lett. 6, 161.

Xiaofei Dong, Jianping Xu, Shaobo Shi, Xiaosong Zhang, Lan Lia,, Shougen Yin: Electroluminescence from ZnCuInS/ZnS quantum dots/poly(9- vinylcarbazole) multilayer films with different thicknesses of quantum dot layer, Journal of Physics and Chemistry of Solids 104 (2017) 133–138.

Beilei Yuan, Lianfeng Duan, Qiqian Gao, Xueyu Zhang, Xuesong Li, Yue Yang, Li Chen, Wei Lü: Investigation of metal sulfide composites as counter electrodes for improved performance of quantum dot sensitized solar cells, Materials Research Bulletin 100 (2018) 198–205.

Hamid Kazemi Hakki , Somaiyeh Allahyari , Nader Rahemi , Minoo Tasbihi: The role of thermal annealing in controlling morphology, crystal structure and adherence of dip coated TiO2 thin film on glass and its photocatalytic activity , Materials Science in Semiconductor Processing 85 (2018) 24–3.

J.I. Contreras-Rasc´on , J. Díaz-Reyes , A. Flores-Pacheco , R. Lozada Morales , M. E. ´Alvarez-Ramos , J.A. Balderas-L´opez,: Structural and optical modifications of CdS properties in CdS-Au thin films prepared by CBD, Results in Physics 22 (2021) 103914.

S. Mathew, A.K. Prasad, T. Benoy, P.P. Rakesh, M. Hari, T.M. Libish, P. Radhakrishnan, V.P.N. Nampoori, C.P.G. Vallabhan: UV-visible photoluminescence of TiO2 nanoparticle prepared by hydrothermal method, J. Fluoresc 22 (2012) 1563–1569.

H. Chen, D. Chen, L. Bai, K. Shu: Hydrothermal synthesis and electrochemical properties of TiO2 nanotubes as an anode material for lithium ion batteries, Int. J. Electrochem. Sci. 13 (2018) 2118–2125. Y.F. Chen, C.Y. Lee, M.Y. Yeng, H.T. Chiu, The effect of calcination temperature on the crystallinity of TiO2 nanopowders, J. Crystal Growth. 247 (2003) 363–370.

Q. Chen, H. Liu, Y. Xin, X. Cheng: TiO2 nanobelts: effect of calcination temperature on optical, photo electrochemical and photocatalytic properties, Electrochemic Acta 111 (2013) 284–291.

X. Dai, Z. Zhang, Y. Jin, Y. Niu, H. Cao, X. Liang, L. Chen, J. Wang, X. Peng: Solution-processed, high-performance light-emitting diodes based on quantum dots, Nature 515 (2014)96–99.

K.-H. Lee, C.-Y. Han, H.-D. Kang, H. Ko, C. Lee, J. Lee, N. Myoung, S.-Y. Yim, H. Yang: Highly efficient, color-reproducible full-color electroluminescent devicesbased on red/green/blue quantum dot-mixed multilayer, ACS Nano 9 (201510941–10949).

A. Jana, K.N. Lawrence, M.B. Teunis, M. Mandal, A. Kumbhar, R. Sardar: Investigating the control by quantum confinement and surface ligand coating of photocatalytic efficiency in chalcopyrite copper indium diselenide nanocrystals, Chem. Mater. 28 (2016) 1107–1120.

J. Kwak, W.K. Bae, D. Lee, I. Park, J. Lim, M. Park, H. Cho, H. Woo, D.Y. Yoon, K. Char, S. Lee, C. Lee: Bright and efficient full-color colloidal quantum dot lightemitting diodes using an inverted device structure, Nano Lett. 12 (2012) 2362–2366.

M.A. Abbas, M.A. Basit, T.J. Park, J.H. Bang: Enhanced performance of PbS sensitized solar cells via controlled successive ionic-layer adsorption and reaction, Chem. Phys. (2015).